Experimental characterization and numerical modeling of short-glass-fiber composite for vibroacoustic applications

Mehdi Zerrad, Nicolas Totaro, R.G. Rinaldi, Benjamin Eller

Experimental characterization and numerical modeling of short-glass-fiber composite for vibroacoustic applications

M. Zerrad[1], N. Totaro[1] , R.G. Rinaldi[2], B.Eller[3]
[1] LVA, INSA Lyon,
25 bis Avenue Jean Capelle, 69621 Villeurbanne, France
e-mail: **mehdi.zerrad@insa-lyon.fr**

[2] MATEIS, INSA Lyon,
Bât. B. Pascal, 5ème étage - 7, avenue Jean Capelle, 69621 Villeurbanne, France

[3] Renault,
1 Allée Cornuel, 91510 Lardy, France

Abstract
In order to design vehicles with diminished CO_2/km emissions level, car manufacturers -among alternatives- aim at reducing the weight of their vehicles. One of the solutions pursued consists in the replacement of metallic structural parts by light weight polymer based composites ones. Naturally, with these new parts, NHV (Noise, Vibration and Harshness) engineers now face the challenge to predict their vibrational responses. In the present study, focusing on PA6 reinforced glass fiber oil pan, mechanical and microstructural characterizations, dynamic mechanical analysis (DMA) and X-ray tomography measurements respectively were performed and evidenced that the complex modulus of the parent material not only depends on temperature and frequency but also on humidity content and loading direction. The effect of temperature and humidity content was also evidenced on the vibratory response of the oil pan. Further experimental (modal analysis) and numerical (finite element modeling) comparisons up to 2000 Hz were conducted, showing that simplistic material's descriptions are not satisfactory.

1 Introduction

To diminish the ecological impact of their vehicles accordingly to new legislation, car manufacturers -among alternatives- aim at reducing their weight. One of the solutions advocated by the NVH (Noise, Vibration and Harshness) engineers is the replacement of metallic materials in structural parts by light weight polymer based composites. However, the use of these materials confronts engineers to the challenge of mastering their vibration and acoustic modeling taking into account the complex features of these new constitutive materials. Indeed, the mechanical performance of these composites depends on the intrinsic properties of the constituents (matrix and fillers), their respective volume fractions and various microstructural parameters such as the shape factor, dispersion and arrangement of the reinforcing fillers [1]. Here, the Young's modulus and the loss factor (damping) of Polyamide 6 filled with 35% by mass short glass fibers (denoted PA6-GF35 hereafter) depend on temperature [2], frequency [3], moisture [4], and the distribution of lengths and fiber diameters [4,5], their volume fractions [2] and their orientations [6].

Thus, our study focuses on the characterization of the various microstructural parameters of PA6-GF35 and on the understanding of their impact on the macroscopic vibration behavior of an automobile oil pan. More precisely, the effects of frequency, temperature, moisture and imposed loading in relation to the fibers' orientation on the complex modulus of the material is investigated. Consequently, the influence of temperature and moisture level on the vibratory response of the structure is also pursued. Finally, experimental and numerical modal analyses of the oil pan over a frequency range from 0 Hz to 2000 Hz are performed and compared, showing that a simple model with a constant complex Young modulus can be considered valid only at low frequencies (below 600 Hz). Longer term, the aim of this study is to assess the degree of accuracy required for the constitutive law to propose a persuasive test/calculation confrontation

and use analytic predictive model such as the Cox-Krenchel model which allows to predict the Young's modulus with account for the microstructural parameters previously mentioned.

1.1 System under study: PA6-GF35 oil pan

The oil pan illustrated in figure 1 is a PA6-GF35 injection-molded part. The structure is constituted by a "main structure" assimilated to the general shape of the part, and numerous ribs that are stiffening the structure. Figure 1a also shows that the oil pan contains a metal tube and metal rings inserted in ten holes which are used to assembly the oil pan with the block cylinder. Dried, the part weighs 995.4 g including the aforementioned metal parts ($m_{\text{filter fixation}} = 110$ g and $m_{\text{rings}} = 38$ g).

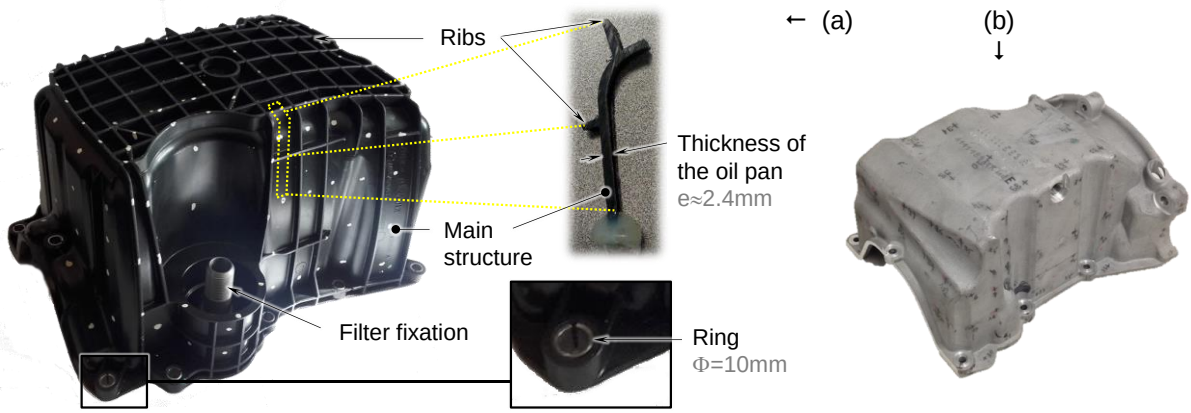

Figure 1: (a) PA6-GF35 oil pan. The bottom right image shows the mounted metal rings. The top right image highlights a section of the "main structure" and ribs from a cutting element of the oil pan. (b) Aluminum oil pan (*N.B.* both images are not on the same scale).

2 Effect of temperature on the PA6-GF35

2.1 Effect of temperature on the vibration behavior of the structure

To assess the impact of temperature on the PA6-GF35 oil pan, transfer function measurements were carried out for four different temperatures: 20°C, 50°C, 80°C and 110°C (the latter being the operating temperature of the oil pan in the vehicle). The oil pan has been previously dried at 80°C under vacuum and measurements were performed for a constant humidity content of about 0.3%. The oil pan was suspended by an elastic link in an INSTRON® thermo-regulated chamber and the vibration measurements were performed using an impact hammer (average on five impacts) over a frequency range 0 Hz to 2000 Hz on a single measurement point randomly yet conveniently chosen.
Figure 2 shows that the higher the temperature, the lower the natural frequencies. The observed offsets are limited to few Hz at low frequency but can exceed 100 Hz above 500 Hz. This means that the increase of the temperature decreases the Young's modulus of the constitutive material. In addition, the damping is highly increased as can be seen at resonance peaks in Figure 2.

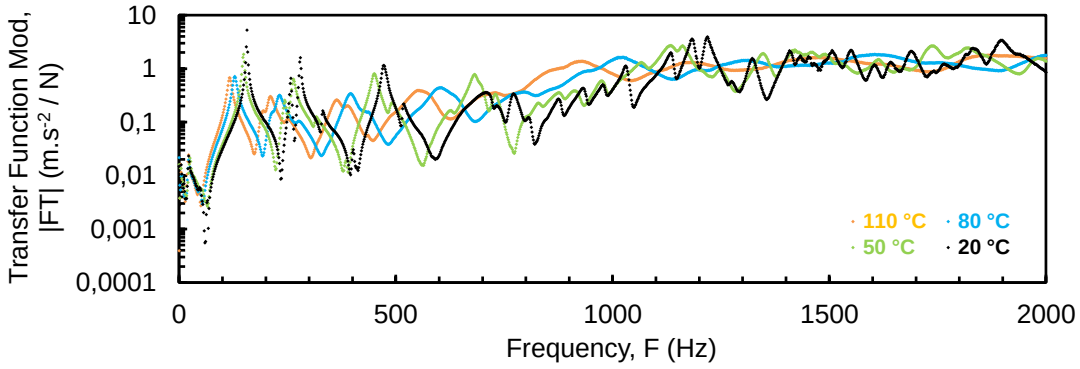

Figure 2: Effect of temperature on the transfer functions (acceleration over force) of the PA6-GF35 oil pan.

The variabilities of these measurements are only due to variations of the material properties. Indeed, a reproducibility study involving 4 operators was conducted to evaluate the influence of both the mounting and the operator on the measured transfer functions. The results are presented in Figure 3 showing that the four transfer functions of the four operators overlap over the entire frequency range investigated.

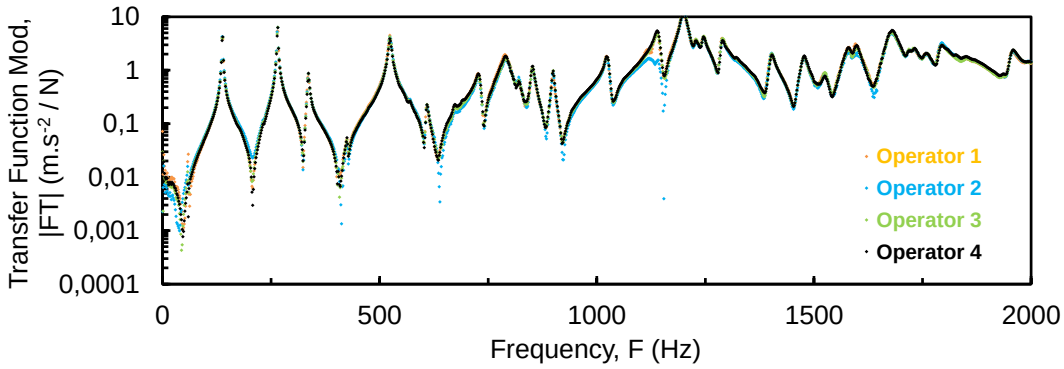

Figure 3: Transfer functions obtained by four different operators on the PA6-GF35 oil pan at a constant temperature (T_{amb}) and moisture.

To highlight the effect of temperature on the PA6-GF35 part, transfer functions measurements were also carried out on an aluminum oil pan ($m_{\text{Aluminum oil pan}} = 2.68\,\text{kg}$) for the same temperature range. The results are reported in figure 4 showing that the temperature has a slight impact on the aluminum oil pan

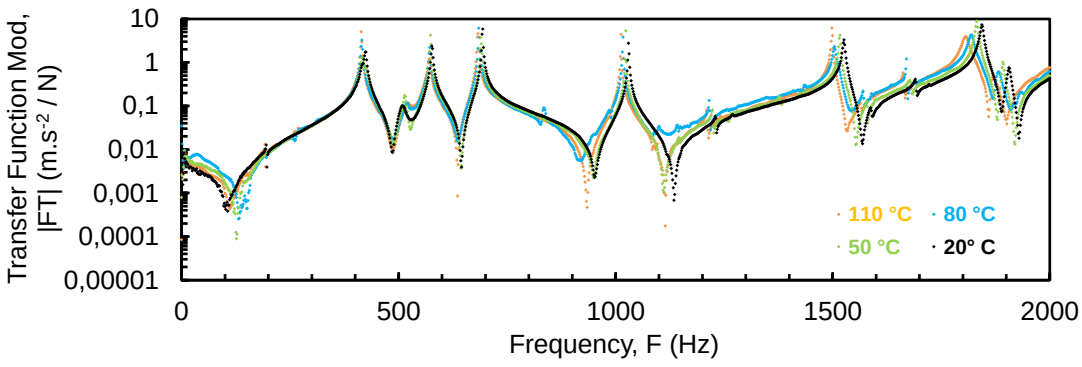

Figure 4: Effect of temperature on the transfer functions (acceleration over force) of the aluminum oil pan over a frequency range from 0 Hz to 2000 Hz.

More precisely, slight shifts of the resonance peaks to lower frequencies can be observed when increasing the temperature, with the offset increasing as the resonance frequency increases; for instance, above 1000 Hz, the offset is about 10 Hz. The curves also allow to observe that, close to 2000 Hz, peaks are more damped for higher temperatures. However, when comparing Figure 4 and Figure 3, it is clear that even if the trends are the same for both parts, meaning the decrease of the Young modulus and increase of the damping of the parent materials, the effect of temperature is more pronounced for the PA6-GF35.

2.2 Effect of temperature on the viscoelastic properties of the PA6-GF35

Dynamic Mechanical Analysis (DMA) were used to measure the complex modulus E* for prescribed frequencies and temperatures. Practically, a small amplitude sinusoidal loading displacement is imposed to the sample and the force signal, also sinusoidal but shifted, is measured. From both signals, the storage modulus E' (assimilated to the Young's modulus and denoted E hereafter), the loss modulus E'' and the loss factor tanδ can be computed. They relate to the complex modulus E* as follow:

$$E^* = E' + i\,E'' = E'\,(1 + i\tan\delta) \tag{1}$$

DMA analysis in three-point bending was performed on a cuboidal sample of dimensions 2.3 x 4.7 x 20 mm^3 and humidity content of 1.4%. The specimen was cut in the "main structure" of the oil pan and tested without prior treatment. Three frequencies (0.2 Hz, 1 Hz and 5 Hz) were tested for temperatures ranging from 0°C to 150°C (the engine operation temperature being 110°C). The results are reported in Figure 5 where the changes of the Young's modulus (see a) and loss factor (see b) as a function of temperature are shown for the three frequencies listed above. The higher the temperature the lower the Young's modulus, decreasing from a maximum value of 9000 MPa at 0°C to about 3000 MPa to 150°C.

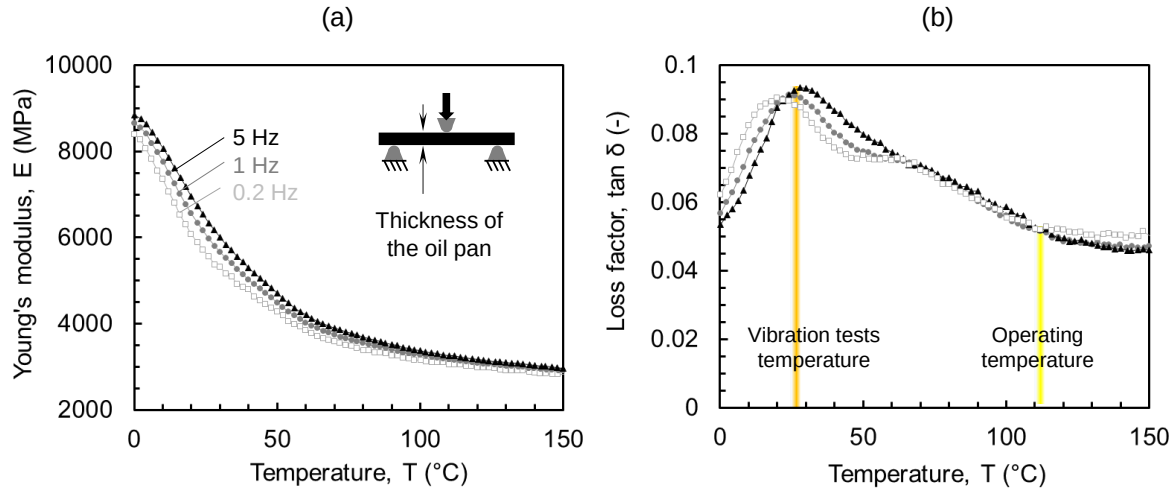

Figure 5: Young's modulus and the loss factor as a function of temperature and frequency obtained by DMA on a PA6-GF35 sample cut from the oil pan.

The maximum damping, often identified as the glass transition temperature T_g of the PA6 matrix (at 1Hz), is located at about 25°C, shifting towards higher temperature when the loading frequency increases. The temperature measured here is characteristic of PA6 materials plasticized by water [7].
The evolution of the Young's modulus with temperature obtained by DMA confirms the observations made previously about the impact of temperature on the vibrational response of the PA6-GF35 oil pan, justifying why the measured natural frequencies are shifted to lower frequencies and why the damping is increased when the tested temperature is increased.

3 Effect of humidity content on the PA6-GF35

3.1 Effect of humidity content on the vibration behavior of the structure

In order to understand the effect of humidity content on the vibration behavior of the oil pan of PA6-GF35, transfer function measurements were performed at ambient temperature for three humidity contents. To do so, the oil pan was dried in air at 70 ° C for 10 days to reach a humidity level close to 0 %, and subsequently immersed in a water bath for two weeks to get a significant humidity content. The evolution of the humidity content has been followed by weighing the oil pan. Finally, measurements were carried out for humidity contents of 0.4%, 3.1%, and 5.2%. The results presented in Figure 6 show that humidity content has a significant influence on the vibration behavior of the PA6-GF35.

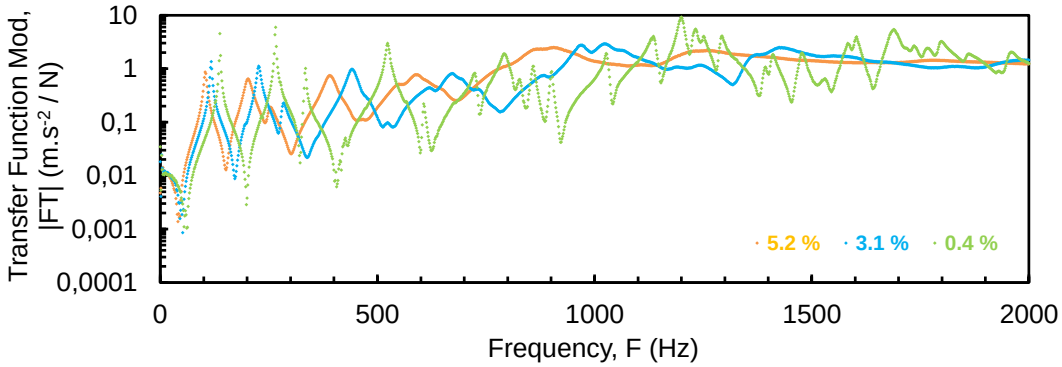

Figure 6: Transfer functions (acceleration over force) of the PA6-GF35 oil pan for three different levels of moisture: 0.4%, 3.1% and 0.4%.

It can be noticed that the higher the humidity content in the material the more the natural frequencies are shifted to lower frequencies with an offset greater than 100 Hz above 200 Hz. In other words, the lower the humidity content, the greater the stiffness of the part, i.e. the greater the Young's modulus of the parent material)

We can also notice that damping is greater at high humidity. Indeed, figure 6 shows that for the transfer function measured at 5.2% of humidity the resonance peaks disappear completely above 1000 Hz. It is worth noting that moisturized PA6-based materials exhibit their glass transition temperature T_g around room temperature (as already discussed with the DMA results in Figure 5b, here coinciding with the testing temperature [8]).

3.2 Effect of humidity content on the parent material

To further evidence the importance of the humidity content on the mechanical performance of PA6-GF35 around ambient temperature, the humidity content was changed on one sample and the complex modulus measured by DMA. The various states are obtained by drying (vacuum oven) and immersion in water bath, and the content was monitored by weighing the specimen. Furthermore, the weighing was performed before and after each test to confirm that the humidity content remained constant throughout the test.
Figure 7 shows the evolution of the Young's modulus as a function of the humidity content between 30 ° C and 70 ° C.

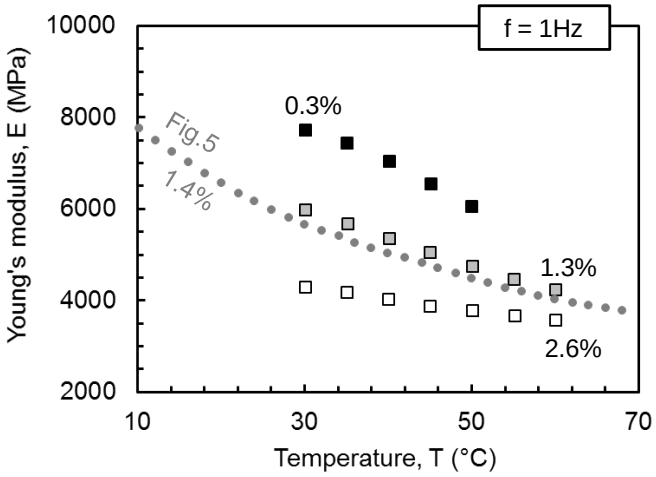

Figure 7: Young's modulus measured by DMA as a function of the moisture level (percent values next to the curves) and temperature at 1 Hz.

The study shows that the Young's modulus decreases when the humidity content increases; at 30°C, the modulus drops from 8000 MPa for the driest case (0.3% moisture) to 4200 MPa for the most waterlogged case (2.6% moisture).
The DMA results are consistent with the vibration behavior of the PA6-GF35 part when the PA6 matrix is dried, its glass transition temperature T_g is around 50°C [9], so the more the material is wet the more its glass transition temperature is shifted to the low temperature. In the case of this study, the curves in figure 6 has been measured at ambient temperature, so the loss factor (damping) increases when moisture level increases (Figure 5).

4 Effect of the glass fiber on the viscoelastic properties of the PA6-GF35

4.1 PA6-GF35 microstructural characterization

X-rays tomography is a non-destructive 3D imaging technique which allows to observe a material microstructure at the micron scale.
The sample is positioned between the source and the detector so that the gray level of a reconstructed 2D image reflect differences in absorption of X-rays. In the case of PA6-GF35, this technique is particularly suited for dissociating the fibers from the matrix and thus study the geometrical properties of these last. Here, a 2.5x2.5x2.5xmm^3 volume of material located in the main structure has been imaged at 2 microns resolution.
Figure 8 shows a series of images illustrating the sizes, orientations and dispersion of fibers (white elements) in this limited volume of material. It should be noted that the planes 3 and 4 display sections of the all thickness of the oil pan. Images 1 and 2 correspond to planes parallel to the mold surface, and reveal that approaching the free surface (the surfaces contacting the mold during the injection step), the fibers are relatively randomly oriented in the plane parallel to the mold surface. The fibers' orientations are typical of injection molded parts, where the mold promotes cooling and solidification of the fibers in a disordered state [1].
The Comparison of images 3 and 4 highlight a higher fiber density near the center of the thickness, also a consequence of the injection process [6]. The evolution of the through-thickness fiber concentration is also qualitatively observed in images 1 and 2, the density of fibers being substantially greater in the central region (e/2). To quantify the fiber content and its variations, the images are "thresholded" to separate the matrix (dark voxels) from the fibers (light voxels) and FIJI © algorithm [10] has been used to calculate the corresponding volume fraction of fibers with respect to the 3 main directions of the cubic scanned region.

Finally the fiber volume fraction with respect to the relative position along the 3 axis are calculated and displayed in figure 8b. The profiles are homogeneous and uniform for the two directions collinear to the surface of the mold. Conversely, the fiber density varies depending on the position along the thickness, in accordance with the qualitative observations made in figure 2a. In the scanned volume, the average volume fraction of fibers is approximately 0.2, which is in agreement with the mean mass fraction (35%).

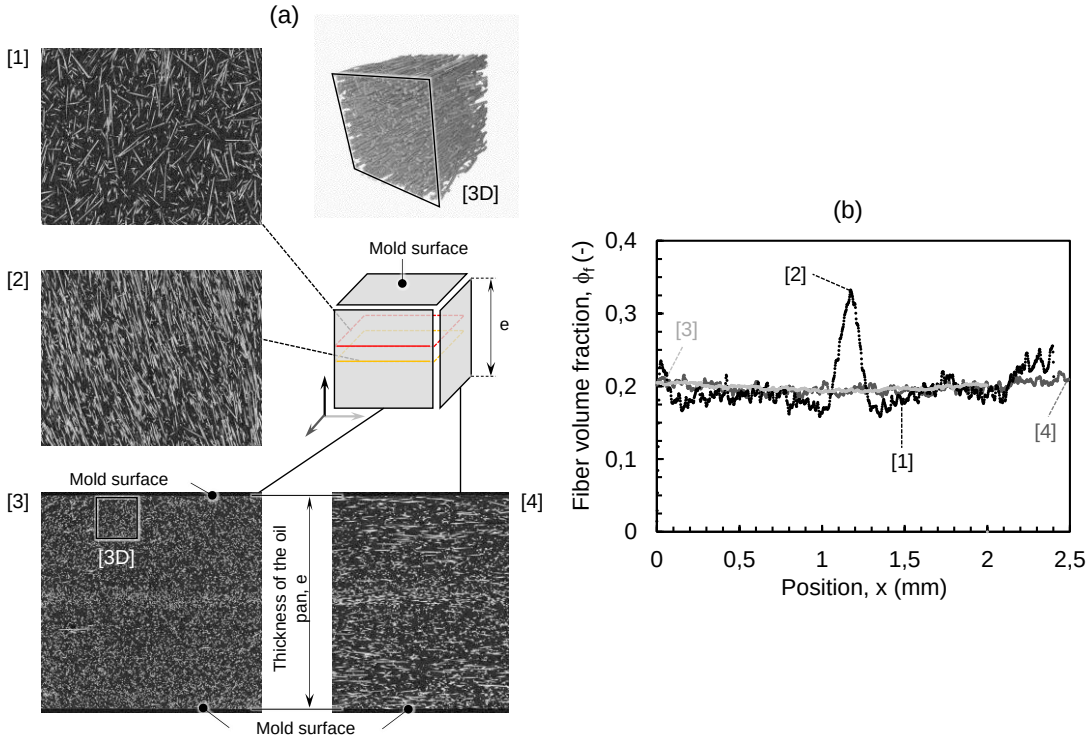

Figure 8 : (a) Tomography X-rays images of a sample cut from the oil pan and a 3D reconstruction of a volume of glass fibers near the surface of the mold with a dimension of 500x500x500 μm^3 (Voxel size = 8 μm^3). (b) Glass fibers volume fractions in the 3 main directions of the scanned volume. N.B. Grayscale curves coincide with the color code of the axis system schemed in (a).

The X-rays tomography also allows to reconstruct a 3D image of the material (see inset in figure 8a). Such reconstruction, performed close to the free surface, confirms that the fibers are oriented in a preferred direction: the direction of the material's flow during the injection, suggesting an anisotropic behavior, studied in the following.

4.2 Mechanical anisotropy of a PA6-GF35 sample

Tests were conducted to test the hypothesis of mechanical anisotropy suggested by the X-ray study of the microstructure. More specifically, DMA measurements in bending mode were performed on the same sample along two preferred directions which are detailed in Figure 9a.

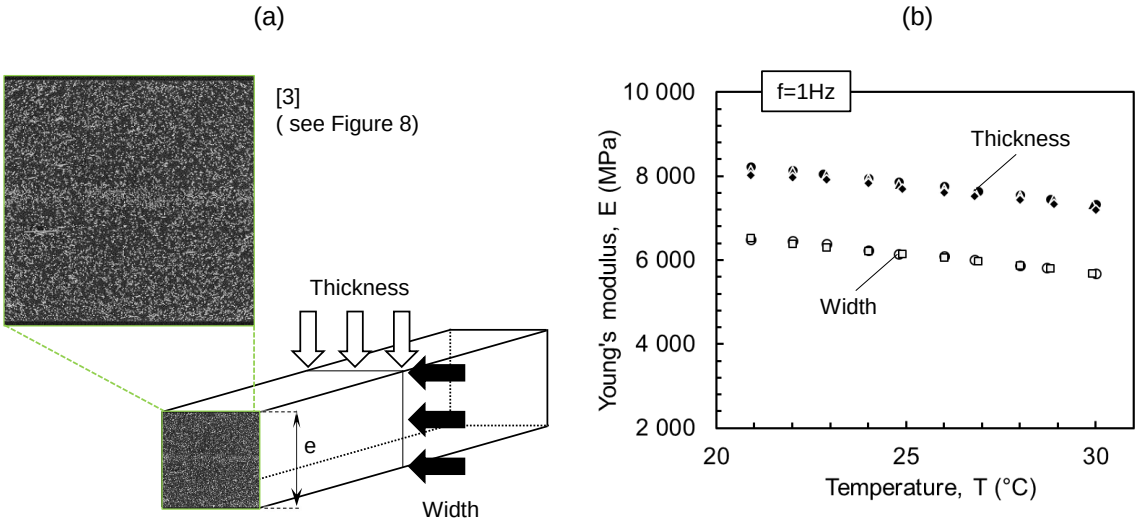

Figure 9: (a) 3-points bending tests, and illustration of the arrangement of fibers relative to the loading. (b) Effect of orientation of the loading on the Young's modulus measured in 3-points flexion by DMA. Several measurement series demonstrate the repeatability of measurements.

The comparison between the Young's modulus measured in the vicinity of ambient temperature is given in figure 9b. A difference of about 2000 MPa is observed, corresponding to a relative change of about 30%, confirming the anisotropy of PA6-GF35. It is worth noting that testing two samples aligned or perpendicular to the major fibers orientation axis should lead to greater discrepancies.

5 Modal analysis test/calculation correlation of the PA6-GF35 oil pan and moisture influence

5.1 Experimental modal analysis

An experimental modal analysis was performed on a PA6-GF35 oil pan. The measurements of the acceleration/force transfer functions were made on a frequency range of 0 Hz to 2000 Hz with the oil pan suspended by an elastic link. A fixed accelerometer was mounted on a measuring point and impacts have been applied on the 182 points of the oil pan. The measurements were conducted at an average temperature of 27 °C .The mass of the oil pan was 1005 g comprising the mass of the tube (110 g) and the metal inserts (38.6 g). Measurements were post-processed using the PULSE B & K software to extract the natural frequencies and modes shapes using a modal analysis algorithm.

5.2 Numerical modal analysis

5.2.1 Cox-Krenchel model

The Cox-Krenchel model has been suggested to predict the Young's modulus of short fiber composite with account for the reinforcement specificities (orientation, concentration, aspect ratio …). In our case, with the composite, the matrix and the fibers depicted with the subscripts PA6-GF35, PA6 and f respectively, the modulus of the composite is expressed as follow:

$$E_{PA6-GF35} = \eta_0 \nu_f E_f \left(1 - \frac{\tanh(ns)}{ns}\right) + (1 - \nu_f) E_{PA6} \quad (2)$$

$$n = \sqrt{\frac{2E_{PA6}}{E_f(1-\nu_{PA6})\ln\left(\frac{1}{\nu_f}\right)}} \quad (3)$$

$$s = \frac{L_w}{d} \quad (4)$$

where η_0 is the orientation factor which varies between 0.3 (random fiber orientation) to 1 (fibers oriented in the same direction). ν_f, L_w and d correspond to the fiber volume fraction, the average length and the average fiber diameter respectively. These quantities can be measured after pyrolysis of the composite and observation of the remaining fibers with a scanning electron microscope (SEM). Naturally, the frequency, temperature and moisture dependencies of the Young's modulus evidenced experimentally are integrated in the matrix Young's:

$$E_{PA6} = f(\text{temperature}, \text{frequency}, \text{moisture})$$

Since the purpose of this work is to identify the level of sophistication necessary to model the complex Young modulus of the system to obtain a good calculation/test correlation, the numerical simulations were performed with the most simplistic numerical model with a homogeneous isotropic Young's modulus, as detailed in the paragraph below.

5.2.2 Correlation with homogenous isotropic Young's modulus

The numerical modal analysis of the oil pan was performed on a frequency range of 0 Hz to 2000 Hz. The Poisson's ratio used is ν = 0.33 and the density is ρ = 1400 kg/m^3, consistent with experimental measurements. Three Young's modulus obtained by DMA and corresponding to three different humidity levels (see Figure 7 and Table 1) were used for calculations in order to see the influence of humidity content on the modal analysis correlation.

The modulus E=5550 MPa corresponds to the temperature and humidity conditions under which the vibration test was performed.

Moisture (%)	Young's modulus (MPa)
0.3	7545
1.3	5550
2.6	4064

Table 1: DMA Modulus of the PA6-GF35 for different humidity content.

The oil pan was meshed with parabolic tetra elements and 534717 degrees of freedom. The metallic tube and rings were modeled with punctual mass elements CONM2 with mass values of 110 g for the filter attachment tube and of 3.86 g for each ring respectively. The calculation was performed using the finite element code Nastran©.

The MAC (Modal Assurance Criterion) index is used to assess the mode shapes calculation / test correlation. A MAC value of 1 indicates a perfect correlation between experimental and numerical mode shapes. Conversely, a value of 0 indicates a non-existent correlation. It is commonly accepted that the correlation is satisfactory for a MAC index higher than 0.8.

The comparison between the measured modes and computed ones are presented in Figure 10. Modeling the oil pan with a homogeneous isotropic modulus obtained by DMA yields a good test/calculation correlation only at low frequency (below 600 Hz). From 600 Hz to 1500 Hz, the mode shapes are mostly undetected or

less correlated, indicating that the numerical model solely consisting of an isotropic fixed Young's modulus is too simplistic compared to the anisotropic and frequency dependent behavior evidenced in the above.

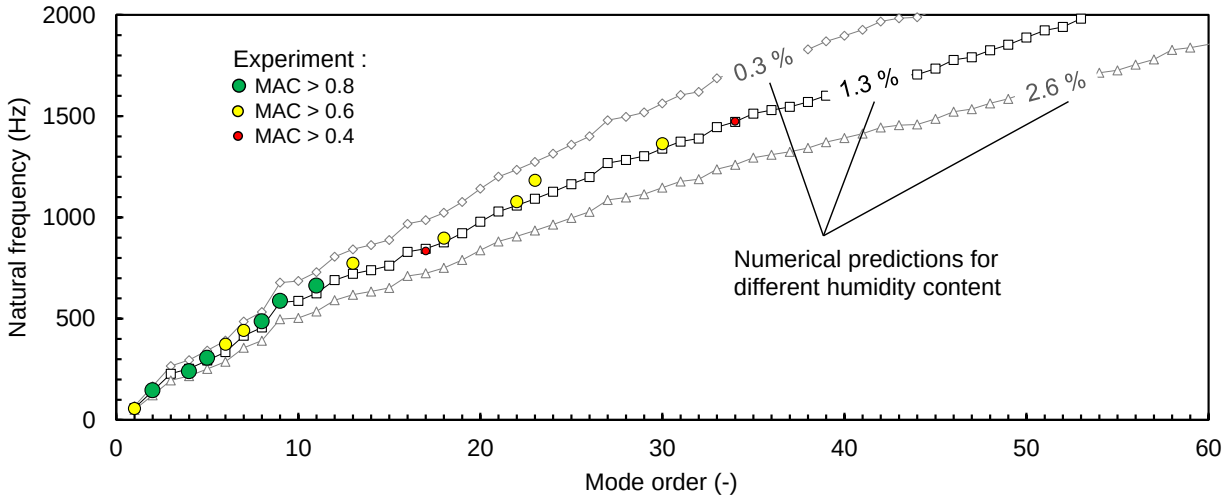

Figure 10: Modal analysis calculation/test correlation of the PA6-GF35 for three different Young's modulus at three different moisture level: triangles: E=4064 MPa; squares: E=5553 MPa; diamonds: E=7545 MPa. Colored circles represent the experimental eigen-frequencies (size of the circle represent the degree of correlation between numerical and experimental mode shapes, biggest is best).

It is also observed that from 600 Hz to 1500 Hz mode shapes are mostly undetected or less correlated, indicating that the experimental modal analysis does not help, as such, to conclude the representativeness of a numerical model with such a Young's modulus, simplistic compared to the reality of the material behavior, evidenced as anisotropic and frequency dependent in the above.

The calculations with Young's modulus corresponding to the moisture contents of 0.3% and 2.6% show the same trend and confirm the impact of the moisture on natural frequencies of the oil pan: the natural frequencies of the wettest cases are lower than those of the dry case, justified by an important decrease of the parent material's modulus.

Finally, it will therefore be necessary to refine the model in order to approach the reality, with taking into account the effect of the frequency and the anisotropy of Young' modulus [11]. Obviously, the damping frequency dependency has to be considered as well.

Conclusion

In this study the impact of temperature and humidity on the vibration response of the PA6-GF35 oil pan has been evidenced and discussed/justified by studying the effect of these parameters on the mechanical behavior of the constitutive composite material. Indeed, the PA6-GF35 material was characterized and a "multi-layer" structure leading to heterogeneous Young's modulus depending on the geometry and more specifically the thickness (a consequence of reinforcing fillers) evidenced.

The low frequency room temperature Young's modulus obtained by DMA for a prescribed humidity content was used as an input in a calculation of numerical modal analysis and allowed performing a comparison with the experimental modal analysis. It was found that natural frequencies and mode shapes test/calculation correlation is relevant up to a frequency of 600 Hz. However, at higher frequencies the small number of modes detected by experimental modal analysis does not allow the observation of the oil pan vibrational behavior between and 600 Hz and 2000 Hz. In addition, modal analysis calculations were performed for two Young's moduli corresponding to two different humidity contents to evidence the strong effect of the contained humidity on the vibrational response of the structure.

Frequency response test/calculation correlations have to be made to get a more accurate correlation at mid frequency. Also, taking into account the frequency dependence of the matrix (for both the modulus and the

damping) and the materials anisotropy resulting from the fibers orientation have now to be considered to model in a more relevant manner the real behavior of the short fiber reinforced polymer based composite [12], and ultimately the vibration response of the pan. To do so, the use of the Cox-Krenchel shear lag model is currently pursued.

Acknowledgements

This work was performed within the framework of the Labex CelyA of université de Lyon, operated by the French National Research Agency (ANR-10-LABX-0060/ ANR-11-IDEX-0007).

The authors would like to thank Misses A. Hautier and C. Rougier for their assistance for conducting this study.

References

[1] A. Bernasconi, D. Rossin, C. Armanni, *Analysis of the effect of mechanical recycling upon tensile strength of a short glass fibre reinforced polyamide 6,6*. Engineering Fracture Mechanics 74 (2007): 627-641.

[2] V. Crupi, E. Guglielmino, G. Risitano, F. Tavilla, *Application of Digital Image Correlation for the effect of glass fibres on the strength and strain to failure of polyamide plastics*. In convegno IGF XXII Roma 2013.

[3] I. C. Steffens, D. I. M. Atzler, *Method for Simulating the NVH Behavior of Plastic Materials*.

[4] A. Bernasconi, F. Cosmi, *Analysis of the dependence of the tensile behaviour of a short fibre reinforced polyamide upon fibre volume fraction, length and orientation*. Procedia engineering (2011), 10, 2129-2134.

[5] A. Bernasconi, F. Cosmi, D. Dreossi, *Local anisotropy analysis of injection moulded fibre reinforced polymer composites*. Composites Science and Technology (2008), 68(12), 2574-2581.

[6] J. J. Horst, *Influence of fibre orientation on fatigue of short glassfibre reinforced Polyamide*. TU Delft, Delft University of Technology (1997).

[7] M. I. Ed. Kohan, *Nylon plastics handbook* (Vol. 378). New York: Hanser (1995).

[8] BASF Corporation, *Mechanical performance of polyamides with influence of moisture and temperature – Accurate evaluation and better understanding.*

[9] H. K. REIMSCHUESSEL, Chemical Research Center, Allied Chemical Corporation, Morristown, New Jersey 07960. *Relationships on The Effect of Water on Glass Transition Temperature and Young's Modulus of Nylon 6*.

[10] http://fiji.sc/.

[11] G. Risitano, D. Corallo, F. L. Sellani, A. Davitti, N. Bellato, *Analisi numerica-sperimentale dell'influenza delle caratteristiche elastiche dei materiali compositi sulle proprietà di vibrare.* In Workshop IGF: Problematiche Di Frattura Ed Integrità Strutturale Di Materiali E Componenti Ingegneristici, Forni Di Sopra (UD), 1-3 Marzo 2012 (p. 120). Gruppo Italiano Frattura.

[12] S. Calmels, M. Lesueur, A. Cheruet. *Anisotropic Damping Behavior of Reinforced Plastic Parts for NVH Simulations*. In SPE Automotive Composites Conference & Exhibition (2015).